

Short Communication

Acetic Acid Treatment of Commercial PtRu for Enhancement of Methanol Electrooxidation

Zirong Li^{1,2,*}, Lei Bai² and Baokang Jin^{1,*}

¹ College of Chemistry & Chemical Engineering, Anhui University, Hefei, Anhui, China, 230601

² College of Chemistry and Materials Engineering, Anhui Science and Technology University, Bengbu, Anhui, China, 233000

*E-mail: lizir@ahstu.edu.cn

Received: 13 July 2019 / Accepted: 29 August 2019 / Published: 29 October 2019

Commercial carbon supported platinum-ruthenium alloy (Pt₅₀Ru₅₀) was selected and employed as the target catalyst for the methanol electrooxidation. The performance Pt₅₀Ru₅₀/C in methanol oxidation could be easily enhanced by over 3 times after it was treated in the acetic acid under hydrothermal condition for 2 hours. The structure of this commercial carbon supported platinum-ruthenium alloy was well characterized by X-ray diffraction, transmission electron microscopy and X-ray photoelectron spectroscopy. In addition, the data from inductively coupled plasma optical emission spectrometry confirmed that a loss of Pt and Ru to some extent was observed and however, the molar ratio of Pt and Ru was kept as well as more fine particles were obtained. Our catalytic results suggested that the oxidation of ruthenium was one key point for the enhancement of catalytic ability, possibly due to the fact that after acetic acid treatment, more ruthenium oxides were presented, which could provide more active hydroxyl species and thus enhanced the catalytic ability. The dissolved oxygen in the acetic acid possibly led to the formation of Ru oxides and nearly had effect on the Pt. The present work expected that it could provide a new insight and facile method to increase the performance of commercial electrocatalysts for direct methanol fuel cell.

Keywords: platinum-ruthenium alloy; acetic acid; solvothermal treatment; methanol oxidation

1. INTRODUCTION

Platinum (Pt) based materials are demonstrated to be efficient catalysts in various fields of electrocatalysis.[1-2] However, due to the high cost, the employment of Pt was limited to a large extent. Accordingly, different methods have been developed to reduce the usage of Pt as well as in increase the activity. For examples, the synthesis of alloys is considered to be one promising way and PtCu as well as PtNi with different structures were prepared. [3-5]

Furthermore, PtRu alloys also represent a kind of very important catalysts in direct methanol fuel cell, due to the fact that on the one hand, the presence of Ru species in PtRu alloys could favor the formation of active hydroxyl species with water molecule and on the other hand, easily induce the rupture of H–O bonds adsorbed at the neighboring Pt atom [6-10]. In addition, it was revealed that the RuO_x species in the PtRu alloys could further enhance the methanol oxidation ability in comparison with the metallic Ru, possibly due to the fact that the RuO_x species are more efficient to provide the hydroxyl groups. The mechanism of methanol electrooxidation over PtRu catalysts had been well established as “bifunctional mechanism” [11,12]. Based on the above information, various kinds of PtRu nanomaterials such as alloys, heterostructures and nanodendrites were reported in order to increase the methanol oxidation ability [13,14]. However, in spite of the structure and competent modification, it is still a challenge to improve the performance of PtRu based electrocatalyst, especially the commercially available catalysts with facile methods. Herein, the present work provided a solution for increasing the catalytic activity of commercial Pt₅₀Ru₅₀ as an example by acetic acid, which is cheap and highly available.

2. EXPERIMENTAL

2.1 Materials

The commercial Pt₅₀Ru₅₀/C (Pt 50%, Ru 50%, Atomic wt%) was purchased from Alfa Aesar. Glacial acetic acid was analytically pure.

2.2. Sample preparation

50 mg Pt₅₀Ru₅₀/C was added into 10 mL PTFE-lined reactor with 5 mL glacial acetic acid and then was treated at 393 K for 2 h before cooling to room temperature. The treated sample was washed by ethanol for 3 times by centrifugation and finally dried under vacuum overnight for further use (A-Pt₅₀Ru₅₀/C). The untreated Pt₅₀Ru₅₀/C was used as reference (B-Pt₅₀Ru₅₀/C). 4.0 mg Pt₅₀Ru₅₀ before and after treatment was added into 1.0 mL ethanol with 5% nafion. After ultrasonic treatment for 30 min, a 10 μL dispersion of the sample was drop-cast onto a glassy carbon electrode.

The solutions for Inductively Coupled Plasma Optical Emission Spectrometry were prepared as following: 2.4 mg of the untreated and treated samples were put into a 10 mL PTFE-lined reactor with 3.00 mL aqua regia and then was treated at 413 K for 1 h before cooling to room temperature. All the solutions were diluted to 50.00 mL for the analysis.

2.3 Characterization

X-ray diffraction (XRD) patterns were recorded on XD3, Beijing. X-ray photoelectron spectroscopy (XPS) was performed with a Thermo ESCALAB 250 instrument with a monochromatic Al K α ($h\nu = 1486.6$ eV) X-ray source. The morphologies of the sample were examined by transmission

electron microscopy (TEM), using a JEOL JEM-2010 LaB6 operated at 200 kV. The high-resolution transmission electron microscope was performed on JEOL JEM-ARM200F, which was operated at 200 kV. Inductively Coupled Plasma Optical Emission Spectrometry (ICPAES) analyses were performed in instruments' Center for Physical Science, University of Science & Technology of China.

2.4 Electrocatalytic study

The electrochemical catalytic activities of the samples were studied by using a three-electrode system on a CHI 600 dual channel electrochemical workstation. A platinum wire and an Ag/AgCl (3 M KCl) electrode were used as the counter electrode and the reference. Cyclic voltammetry (CV) was conducted in the supporting electrolyte for multiple cycles until a stable curve was obtained in a 0.5 M H₂SO₄ solution containing 1 M CH₃OH. The CV was performed at room temperature and the potential was swept between -0.2 and 1.2 V at a rate of 50 mV s⁻¹. The chronoamperometry was recorded at a bias voltage of 0.8 V for 2000 s.

3. RESULTS AND DISCUSSION

First of all, the A-Pt₅₀Ru₅₀/C and B-Pt₅₀Ru₅₀/C were analyzed by XRD and the patterns were displayed in Figure 1. As shown, no obvious difference from the patterns was noticed, indicating that the acetic acid treatment did not modify the crystallinity of the sample and no observable leaching of Pt and Ru could be detected. Furthermore, the modification of particle size and composition could not be obtained from XRD and thus, TEM and XPS analysis were performed in the following.

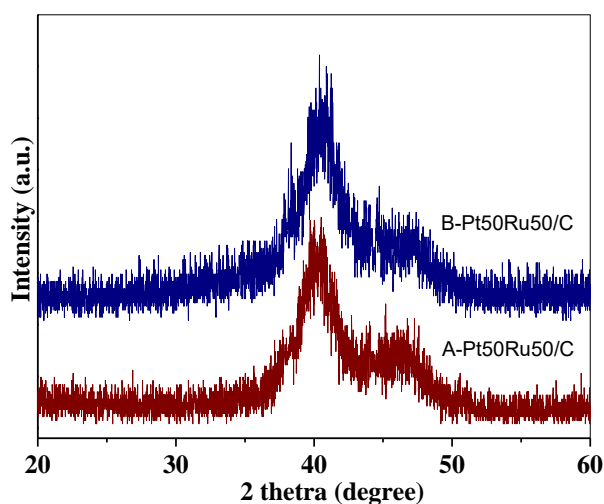


Figure 1. XRD patterns of A-Pt₅₀Ru₅₀/C and B-Pt₅₀Ru₅₀/C.

The morphology of untreated Pt₅₀Ru₅₀ was observed by TEM as shown in Figure 2A. As it can be seen, aggregated particles were presented and the HRTEM image in the inset revealed that the lattice distance was 0.222 nm, which corresponded to the (111) faces. It is worth mentioning that this value was

very close to that reported in the previous work and it is suggested that the ratio between Pt and Ru in the sample is close to 50:50 [9]. After the acetic acid bath, more fine particles were obtained as shown in Figure 2B and the lattice distance of the treated PtRu sample was 0.223 nm, which was nearly the same as the untreated, indicating that the acetic acid did not obviously cause the change of the ratio between Pt and Ru in the alloy.

However, it is important to get an idea about the weight of Pt and Ru in the samples before and after acetic acid to understand the structural modification observed from the TEM. ICPAES results were shown in Table 1.

Table 1. ICP-AES results of the Pt and Ru weight in the A-Pt₅₀Ru₅₀/C and B-Pt₅₀Ru₅₀/C.

State	Pt ($\mu\text{g/mL}$)	Ru ($\mu\text{g/mL}$)	Molar ratio (Pt/Ru)
B-Pt ₅₀ Ru ₅₀ /C	25.67	12.62	1.08
A-Pt ₅₀ Ru ₅₀ /C	17.79	8.15	1.05

Clearly, although a leaching of the Pt and Ru was noticed (7.88 $\mu\text{g/mL}$ for Pt and 4.47 $\mu\text{g/mL}$ for Ru), the ratio of Pt and Ru was nearly not changed.

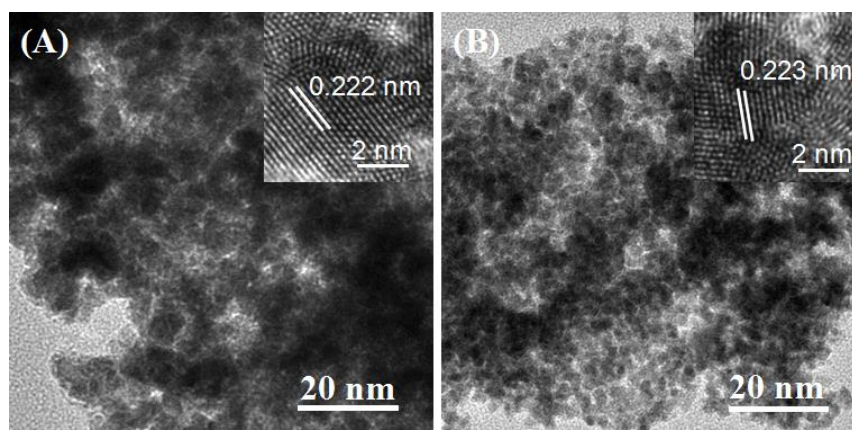


Figure 2. TEM and HRTEM (inset) images of B-Pt₅₀Ru₅₀/C (A) and A-Pt₅₀Ru₅₀/C (B).

More importantly, XPS analysis could provide more useful surface information about the B-Pt₅₀Ru₅₀/C and A-Pt₅₀Ru₅₀/C. As evidenced in previous work [8], ruthenium oxide species is more favorable for producing the active hydroxyl species and thus the chemical state of Ru in B-Pt₅₀Ru₅₀/C and A-Pt₅₀Ru₅₀/C was studied as shown in Figure 3A. It is suggested that before treatment, ruthenium oxide species were observed in the commercial sample as suggested by the peak around 464.5 eV and after treatment, an obvious increase of this peak was clearly observed.

These results strongly confirmed that the acetic acid treatment could lead to the formation of ruthenium oxide on the surface of the sample. It is believed that the modification of ruthenium species could result in the change of the catalytic activity in methanol electrooxidation.[15] Furthermore, after

careful evaluation of the XPS spectra of Pt 4f, no obvious difference was observed, indicating that the acetic treatment did not lead to the formation of platinum oxide as that of Ru. It is worth mentioning that in pure acetic acid, the oxygen dissolved in the acetic acid could result in the formation of Ru oxides and nearly have no effect on the Pt as indicated by the previous work though the condition was different.[16, 17]

Finally, the A-Pt₅₀Ru₅₀/C and B-Pt₅₀Ru₅₀/C were employed as catalysts for direct methanol oxidation. As displayed in Figure 4A, from the CV curves, the electrochemical active surface area (ECSA) of sample B-Pt₅₀Ru₅₀/C and A-Pt₅₀Ru₅₀/C was 16.7 and 39.8 m²mg⁻¹ Pt, suggesting that a higher active surface was reached by acetic treatment. For the CV of methanol in Figure 4B, the B-Pt₅₀Ru₅₀/C showed an onset potential about 0.295 V and this value decreased to 0.235 V after acid treatment, suggesting that an earlier start of methanol was occurred and this result was much better than the commercial Pt/C. In addition, a much higher peak current was obtained by A-Pt₅₀Ru₅₀ (1080 mA mg⁻¹ Pt) in contrast with the A-Pt₅₀Ru₅₀ (325 mA mg⁻¹ Pt) and Pt/C (187 mA mg⁻¹ Pt). Clearly, after acetic acid treatment, the methanol oxidation ability was enhanced by 3.3 times and also was 5.8 times higher than Pt/C as displayed in Figure 4C. The ratio of the intensity of the forward peak/back peak was increased from 1.7 to 2.1 in comparison with 0.93 of commercial Pt/C, also indicating that a better anti-poisoning was achieved by acetic treatment.

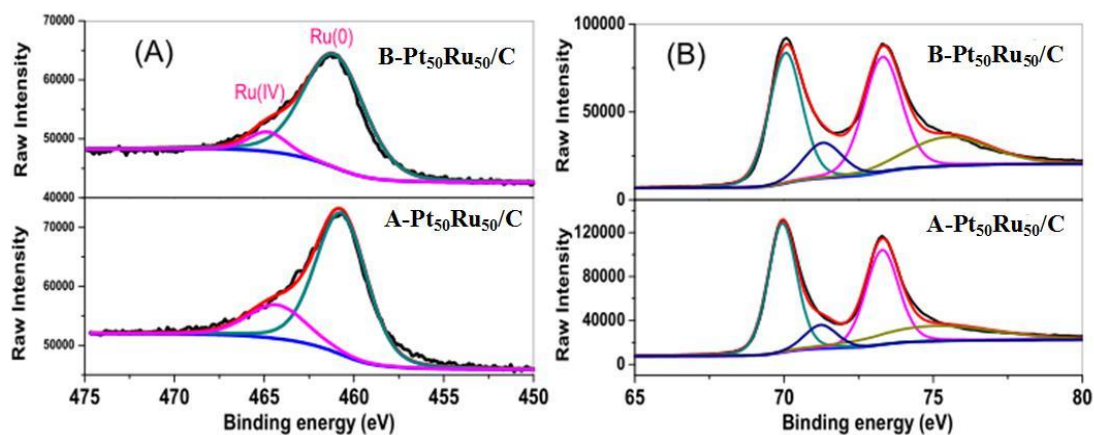
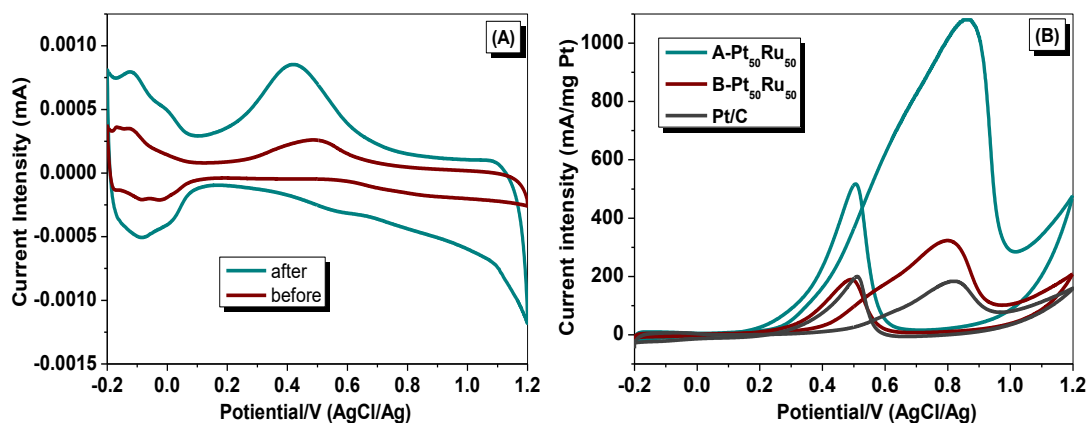


Figure 3. Ru 3p (A) and Pt 4f (B) XPS spectra of A-Pt₅₀Ru₅₀/C and B-Pt₅₀Ru₅₀/C.



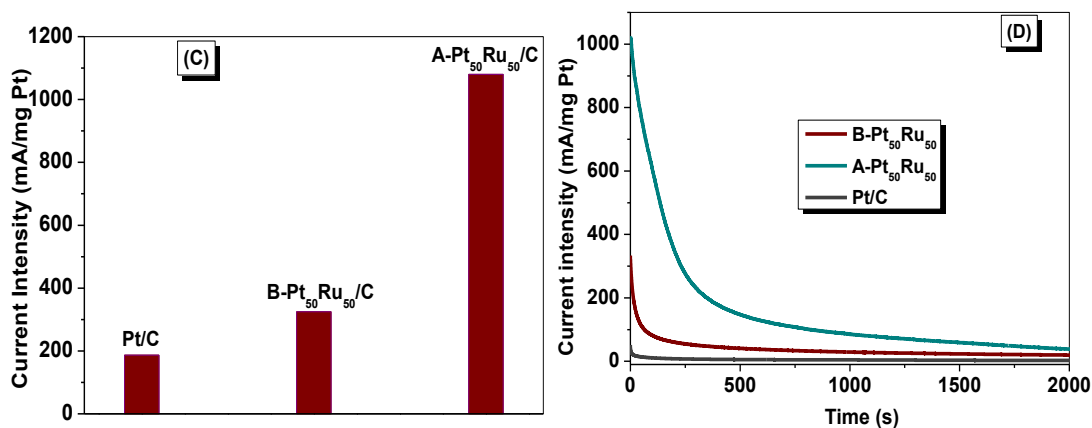


Figure 4. (A) CV of A and B-Pt₅₀Ru₅₀ in 0.5 M H₂SO₄ solution. Scan rate 0.05 V s⁻¹. (B) CV of methanol on A and B-Pt₅₀Ru₅₀ as well as Pt/C in 0.5 M H₂SO₄ + 1 M CH₃OH solution. Scan rate 0.05 V s⁻¹. (C) The comparison of the intensity of the forward peak. (D) Chronoamperometric curves of CH₃OH oxidation at + 0.7 V in 0.5 M H₂SO₄ + 1 M CH₃OH solution on the above samples.

Furthermore, the chronoamperometry was employed to study the electrochemical stability of the three samples. As can be seen from Figure 4D, the A-Pt₅₀Ru₅₀ has a higher starting current intensity compared to the untreated one. At the very beginning, a significant decrease of the current intensity was observed in both case of treated and untreated one. After 2000 s, the current density from the A-Pt₅₀Ru₅₀ is higher (41 mA mg⁻¹ Pt) by the factor of 2 and 6 than those obtained from the B-Pt₅₀Ru₅₀/C (19 mA mg⁻¹ Pt) and Pt/C (7.8 mA mg⁻¹ Pt), further demonstrating the higher electrocatalytic durability of the acetic acid treated Pt₅₀Ru₅₀. In comparison with the synthesized PtRu catalysts as listed in Table 1, the A - Pt₅₀Ru₅₀ was much efficient for the methanol oxidation.

In one word, the methanol electrocatalytic ability of commercial Pt₅₀Ru₅₀ was obviously enhanced by acetic acid treatment under hydrothermal condition for 2 h, possibly due to the fact that more Ru oxide species and fine structure were achieved. The treated sample could be used as potential catalysts for DMFC and this method may be applied in other PtRu catalysts. The influence of the concentration of acetic acid, other acid, the treating time on the catalytic ability of the commercial PtRu as well as the reuse of the Pt and Ru leached into the solution is under investigation in our lab.

Table 1. Comparison of the intensity of the forward peak of methanol oxidation over different PtRu samples.

Samples	Peak intensity (mA/mg Pt)	Refs.
PtRu/PPDA-MWCNTs	731.6	18
PtRu/MWCNTs	440.5	
Ru-Pt/C	483	19
PtRu nanosponges	410	20
PtRu alloys	370	21
Pt ₈₀ Ru ₂₀ /C nanowires	500	22
A-Pt ₅₀ Ru ₅₀	1080	This work
B-Pt ₅₀ Ru ₅₀	325	

4. CONCLUSION

The present evidenced that acetic acid treatment of commercial Pt₅₀Ru₅₀ could lead to an obvious increase of the electrocatalytic ability in methanol oxidation, which possibly due to the fact that more ruthenium oxide species were formed on the surface of the catalyst and fine structure was achieved. This treatment would provide a facile method for treating commercial electrocatalysts and enhancing the electrocatalytic performance.

CONFLICT OF INTEREST STATEMENT

The author declared no conflict of interests.

ACKNOWLEDGMENT

This work was supported by the National Nature Foundation of China (Grant No. 21175001), the Talent Introduction Project of Anhui Science and Technology University (NO.830166), as well as the Open Project (KF201601) of Key lab of Novel Thin Film Solar Cells are greatly appreciated for the financial support.

References

1. (a) F. Lu, C. Y. Zhang, J. H. Cheng, C. Zhu, H. J. Zhang, X. Cheng, *Int. J. Electrochem. Sci.*, 13 (2018) 9007 (b) T. Unmüssig, J. Melke, A. Fischer, *Phys. Chem. Chem. Phys.*, 21(2019) 13555.
2. (a) G. P. Yi, Z. W. Chang, G.Z. Liu, L. M. Yang, *Int. J. Electrochem. Sci.*, 14 (2019) 7232. (b) L. Zhang, K. Doyle-Davis, X. L. Sun, *Energy Environ. Sci.*, 12 (2019) 492.
3. I. Jiménez-Morales, S. Cavaliere, D. Jones, J. Rozière, *Phys. Chem. Chem. Phys.*, 20 (2018) 8765.
4. N.K. Chaudhari, J. Joo, B. Kim, B. Ruqia, S.I. Choi, K. Lee, *Nanoscale*, 10 (2018) 20073.
5. L. Bai, Y. W. Bai, *J. Nanopart. Res.* 20 (2018) 24.
6. D. J. Chen, S. G. Sun, Y. Y. Tong, *Chem. Commun.*, 50 (2004) 12963.
7. L. M. Zhao, S. P. Wang, Q. Y. Ding, W. B. Xu, P. P. Sang, Y. H. Chi, X. Q. Lu, W. Y. Guo, *J. Phys. Chem. C.*, 119 (2015) 20389.
8. C. X. Xu, L. Wang, X. L. Mu, Y. Ding, *Langmuir*, 26 (2010) 7437.
9. M. L. Xiao, L. G. Feng, J. B. Zhu, C. P. Liu, W. Xing, *Nanoscale*, 7 (2015) 9467.
10. D. J. Chen, Y. Y. Tong, *Angew Chem. Int. Ed.* 127(2015) 9394.
11. N. Kakati, J. Maiti, S. H. Lee, S. H. Jee, B. Viswanathan, Y. S. Yoon, *Chem. Rev.*, 114 (2014) 12397.
12. X. W. Teng, S. Maksimuk, S. Frommer, H. Yang, *Chem. Mater.*, 19 (2007) 36.
13. Y. Z. Lu, W. Chen, *Chem. Commun.*, 47(2011) 2541.
14. P. P. Patel, M. K. Datta, P. M. Jampani, D. Hong, J. A. Poston, *J. Power Source*, 293 (2015) 437.
15. L. Bai, *Appl. Surf. Sci.*, 433 (2018) 279.
16. J. Mikulová, J. J. Barbier, S. Rossignol, D. Mesnard, D. Duprez, C. Kappenstein, *J. Catal.*, 251(2007) 172.
17. S. Hosokawa, H. Kanai, K. Utani, Y. Taniguchi, Y. Saito, S. Imamura, *Appl. Catal. B Environ.*, 45 (2003) 181.
18. B. H. Wu, J. J. Zhu, X. Li, X. Q. Wang, J. Chu, S. X. Xiong, *Ionics*, 25(2019) 181.
19. Y. Y. Zheng, H. T. Zhan, Y. X. Fang, J. H. Zeng, H. Liu, J. Yang, S.J. Liao, *J. Mater. Sci.*, 52(2017) 3457.
20. M. L. Xiao, L. G. Feng, J. B. Zhu, C. P. Liu, W. Xing, *Nanoscale*, 7 (2015) 9467.

21. Y. Li, L. Zheng, S. Liao, J. H. Zeng, *J. Power Sources*, 196 (2011) 10570.
22. G. R. O. Almeida, F. E. López-Suárez, L. S. R. Silva, G. F. Pereira, A. Bueno-López, K. I. B. Eguiluz, G. R. Salazar-Banda, *J. Nanosci. Nanotechnol.*, 19 (2019) 795.

© 2019 The Authors. Published by ESG (www.electrochemsci.org). This article is an open access article distributed under the terms and conditions of the Creative Commons Attribution license (<http://creativecommons.org/licenses/by/4.0/>).